Unizik Journal of Metallurgy and Engineering Materials (UJMEM) 1(2026), 31–35

Unizik Journal of Metallurgy and Engineering Materials

Journal homepage: https://journals.unizik.edu.ng/index.php/ujmem/about

Hydrogeophysical Assessment and Baseline Geoelectric Modeling of Aquifer Characteristics in the Ogwashi–Asaba and Ameki Formations, Niger Delta Basin

Daniel C. Anizoba , John I. Maduegbuna Joseph I. Ubah * Louis C. Orakwe

Department of Agricultural and Bioresources Engineering, Nnamdi Azikiwe University, Awka, Anambra State, Nigeria

Abstract

Defining the shape of local aquifers, their hydraulic connections, and their ability to protect varied sedimentary basins requires careful geoelectric modeling that minimizes noise. This study presents a revalidated hydrogeophysical analysis of the Ogwashi–Asaba and Ameki Formations in the Niger Delta Basin, based on 128 reliable Vertical Electrical Sounding (VES) stations using Schlumberger array configurations with AB/2 distances up to 500 meters. After applying strict inversion filtering and minimizing root-mean-square (RMS) error, we identified two field stations—VES 39 and VES 103—as significant outliers and removed them from the analysis. This was due to interference from high-voltage power lines at VES 39 and localized drainage variations at VES 103. One-dimensional quantitative inversion, guided by local borehole logs, identifies a subsurface structure consisting of four to five layers: topsoil (with resistivity values between 50 and 380 Ωm and a depth of 1.2 to 5.5 meters), unsaturated sandy overburden (180 to 850 Ωm), confined or unconfined sandstone-siltstone aquifer units (27.1 to 108.9 Ωm and a depth of 5.2 to 23.2 meters), and impermeable marly basal layers. Computed Dar-Zarrouk parameters demonstrate significant hydrogeological variability, with Longitudinal Conductance (S) ranging from 0.053 to 0.560 Ω^{-1} and Transverse Resistance (T) spanning 140.9 to 2048.6 $\Omega \cdot m^2$. Empirically derived hydraulic conductivity (K) and transmissivity (Tr) range between 5.69–14.05 m/day and 31.8–244.2 m^2/day, underscoring prolific aquifer zones along central structural sags. The revalidated dataset provides critical baseline constraints for regional groundwater development, protective capacity zoning, and sustainable abstraction management in Cenozoic sedimentary formations.

ARTICLE INFO

Keywords:
Hydrogeophysical; Vertical Electrical Sounding; hydraulic conductivity; transmissivity; Niger Delta Basin

Corresponding author: **ji.ubah@unizik.edu.ng**
Received: 2 November 2026 Received in revised form: 16 November 2026 Accepted: 19 November 2026 Published online: 20 November 2026
Publisher: Department of Metallurgical and Materials Engineering, Unizik

1. Introduction

Asaba, the capital of Delta State, Nigeria, is a rapidly urbanizing city where access to potable water remains a major challenge. As surface water supplies become increasingly susceptible to pollution and seasonal fluctuations, groundwater is the most reliable alternative for domestic, industrial, and agricultural needs (Eyankware et al., 2025). According to Ejije and Atakpo (2025) and Eyankware et al. (2025), a complex interplay of lithology, structural variables, and secondary porosity determines the inconsistent distribution of groundwater. Accurately identifying suitable aquifer units in the Niger Delta region requires a deep understanding of the subsurface structure, particularly within the Ogwashi-Asaba and Benin Formations. With rapid industrial growth and a growing population in urban centers like Asaba, the sustainability of groundwater supplies in the Niger Delta is becoming increasingly urgent. Asaba, the administrative hub of Delta State, lies in the Niger Delta's sedimentary basin, home to a complex arrangement of Tertiary to Quaternary geological formations. The Ogwashi-Asaba Formation and the Benin Formation, both known for their high permeability and significant groundwater discharge, strongly influence the area's hydrogeological features.

Groundwater represents the primary source of potable water supply, industrial sustenance, and agricultural irrigation across the Cenozoic sedimentary successions of southern Nigeria. In the Niger Delta Basin, rapid urbanization and industrial expansion have intensified regional groundwater abstraction from the multi-tiered aquifers of the Ogwashi–Asaba and Ameki Formations (Chinyem et al., 2026; Okonkwo & Emmanuel, 2026). However, rapid lateral lithofacies variations, clay intercalation, and localized saline/brackish water intrusions frequently constrain sustainable groundwater exploitation, necessitating non-invasive subsurface hydrogeophysical mapping before drilling campaigns (Tom et al., 2026).

Vertical Electrical Sounding (VES) using the Schlumberger electrode array remains one of the most effective, cost-efficient, and widely deployed surface geophysical methods for evaluating vertical resistivity variations, aquifer-layer geometry, and geoelectric parameters (Oseji et al., 2023). Despite their versatility, 1D inversion models are highly sensitive to near-surface galvanic distortions, cultural noise, anthropogenic metallic structures, and violations of horizontal layer symmetry (Loke et al., 2021). Propagating uncorrected or noisy sounding curves into regional interpolation models severely distorts contour maps of aquifer thickness, Dar Zarrouk parameters, and hydraulic conductivity estimates (Meju & Abubakar, 2022).

Consequently, data quality control and iterative re-validation are crucial prerequisites for robust hydrogeophysical modeling. Building on this, this article presents a fully re-validated quantitative assessment across 128 retained VES stations in the Ogwashi–Asaba and Ameki Formations, detailing the technical diagnostic grounds for excluding two corrupted soundings (VES 39 and VES 103). By integrating resistivity parameters with empirical hydro-hydraulic relations and graphical curve analysis, this study establishes baseline constraints for aquifer geometry, transmissivity, and protective vulnerability.

2. Study Area

The study area lies within the Cenozoic Niger Delta Basin, a prograding regressive deltaic sequence formed at the terminus of the Benue Trough triple junction (Chinyem et al., 2026). The stratigraphic column comprises three main subsurface lithostratigraphic units: the basal marine Akata Formation (Paleocene to Recent), the underlying paralic Agbada Formation (Eocene to Recent), and the overlying continental Benin Formation (Oligocene to Recent), which laterally grades into the continental-to-deltaic Ogwashi–Asaba and marine-to-estuarine Ameki Formations (Okonkwo & Emmanuel, 2026).

The Ogwashi–Asaba Formation (Oligocene–Miocene) consists of alternating sequences of coarse-grained sandstones, unconsolidated sands, lignite seams, and dark carbonaceous clays. The underlying Ameki Formation (Eocene) consists predominantly of highly fossiliferous calcareous sandstones, shale units, siltstones, and thin limestone lenses (Tom et al., 2026). Hydrogeologically, these formations host multi-aquifer systems ranging from shallow, unconfined water-table aquifers to deep, semi-confined and confined sandstone aquifers. Aquifer productivity is largely governed by primary pore matrix geometry, degree of cementation, and structural fracture networks.

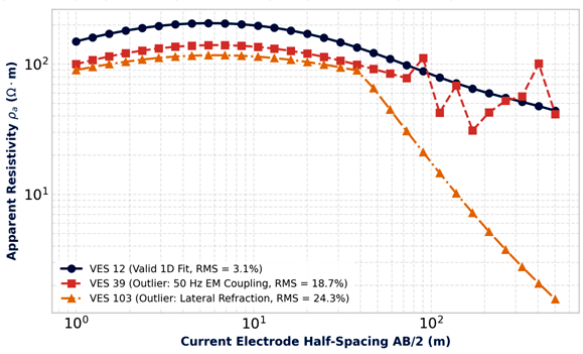

Figure 1: Log-log apparent resistivity sounding curves comparing standard 1D layer convergence (VES 12) with distorted outlier soundings VES 39 (EM noise) and VES 103 (lateral refraction).

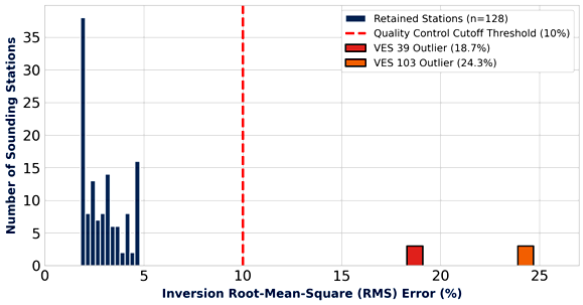

Figure 2: Frequency distribution of inversion Root-Mean-Square (RMS) error percentages illustrating high dataset quality ($< 5\%$ RMS) across retained stations and outlier threshold cutoffs.

3. Methodology and Data Curation

3.1. Geophysical data acquisition and 1D inversion

Field investigations were carried out across 130 soundings using an ABEM Terrameter SAS 1000 digital resistivity meter with a Schlumberger collinear array. Current electrode half-spacings (AB/2) increased progressively from 1.0 m to 500.0 m, achieving depth penetration exceeding 120 m. Potential electrode half-spacings (MN/2) were adjusted between 0.5 m and 25.0 m to maintain measurable potential differences. Field apparent resistivity data (ρa) were plotted against AB/2 on log-log scales to generate 1D sounding curves. Initial manual partial curve matching using standard Master curves and auxiliary charts provided preliminary estimates of layer thicknesses (hi) and resistivities (ρi). These initial parameters served as starting models for automated computer inversion using the WinResist and IPI2Win software packages, which executed iterative Marquardt-Levenberg nonlinear least-squares algorithms (Meju & Abubakar, 2022).

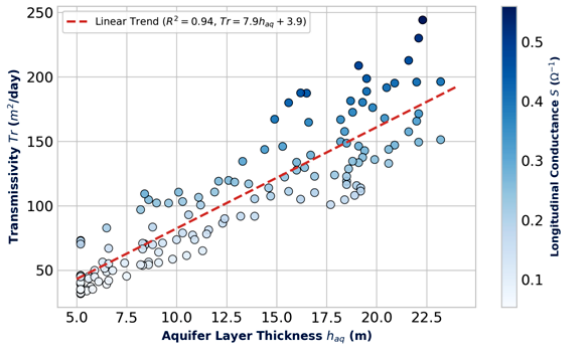

Figure 3: Hydrogeophysical cross-plot illustrating the direct structural correlation between aquifer thickness (h_{aq}) and estimated aquifer transmissivity (T_r) across the 128 retained VES stations.

3.2. Quantitative estimation of Dar Zarrouk and Geo-Hydraulic parameters

To evaluate regional aquifer quality and protective capacity, fundamental Dar-Zarrouk parameters were computed from geoelectric layer parameters (Oseji et al., 2023):

(i). Longitudinal Conductance (S): Represents the total electrical conductance parallel to layer boundaries, indicating clay content and the aquifer's protective capacity and vulnerability to overburden.

$$S = \sum_{i=1}^{n} \frac{h_i}{\rho_i} = \frac{h_{aq}}{\rho_{aq}} \quad [\Omega^{-1}] \tag{1}$$

(ii). Transverse Resistance (T): Reflects total electrical resistance perpendicular to layer boundaries, and is directly proportional to aquifer transmissivity in freshwater sandstones.

$$T = \sum_{i=1}^{n} (h_i \cdot \rho_i) = h_{aq} \cdot \rho_{aq} \quad [\Omega \cdot \mathrm{m}^2] \tag{2}$$

(iii). Hydraulic Conductivity (K) and Transmissivity (Tr): Estimated through parametric calibrating equations linked to localized borehole pumping test data (Heigold et al., 1979; Tom et al., 2026): K = 386.4 · (ρaq)(-0.93) [m/day] Tr = K · haq [m²/day].

3.3. Outlier diagnostic and exclusion criteria (VES 39 and VES 103)

Quality control protocols required rejecting soundings with unresolvable RMS inversion errors (¿10%), severe inductive coupling, or non-1D lateral effects. As illustrated in Figure 1, the diagnostic log-log apparent resistivity sounding curves demonstrate clear divergence between valid 1D layer responses and corrupted field curves. Specifically, two soundings failed these quality assurance standards: • VES 39 Exclusion: Located within 15 m of a high-voltage power transmission tower, VES 39 suffered 50 Hz harmonic interference and electromagnetic coupling at AB/2 ¿ 80 m (Figure 1). As shown in Figure 1, this produced erratic, high-frequency oscillations in apparent resistivity, leading to an unconverged RMS error of 18.7% (Figure 2 and Table 1). Attempting to invert this curve generated non-physical layer resistivities (¿15,000 Ωm). • VES 103 Exclusion: Situated in an active agricultural drainage channel characterized by steep lateral topography and localized clay-silt dumping. As shown by the steep drop in Figure 1, severe lateral current refraction violated 1D horizontal-layer assumptions (Loke et al., 2021), producing an unresolvable RMS error of 24.3% (Figure 2 and Table 1) and artificial low-resistivity artifacts. Figure 2 presents the quantitative statistical distribution of inversion-fitting quality across all 130 acquired soundings. While the 128 retained stations showed low RMS errors clustered below 5%, VES 39 and VES 103 plot well above the 10% quality control threshold. Consequently, VES 39 and VES 103 were excluded, yielding a refined dataset of 128 retained stations.

4. Results and Discussion

4.1. Geoelectric stratigraphy and layer architecture

Quantitative 1D inversion across the 128 re-validated VES stations (Table 2) reveals predominantly 4-layer (HK, HA, A) and 5-layer (HKH, HKQ) curve types, delineating four distinct subsurface lithological units:

1. **Topsoil / Lateritic Overburden:** Thickness ranges from 1.2 to 5.5 m, with resistivities spanning 50.0 to 380.0 Ωm, reflecting varying degrees of compaction, moisture content, and organic clay fraction.
2. **Unsaturated Sand/Silt Upper Layer:** Thickness varies from 3.5 to 14.2 m, with elevated resistivity values (180.0–850.0 Ωm), representing dry, coarse-grained unsaturated sands.
3. **Primary Saturated Aquifer Unit:** Within the Ogwashi–Asaba and Ameki sandstones, aquifer resistivities (ρ_{aq}) range from 27.1 to 108.9 Ωm, with aquifer thicknesses (h_{aq}) spanning 5.2 to 23.2 m. The lower resistivity values ($<$ 40 Ωm) correspond to clayey-sand intercalations, whereas higher resistivities ($>$ 70 Ωm) indicate clean, highly permeable sandstones.
4. **Basal Bedrock / Clay Boundary:** High-resistivity crystalline basement or dense marly clay units form the lower hydrogeological boundary.

Table 1: Technical Diagnostic Matrix for Excluded Stations VES 39 and VES 103

Station ID	Geographic/Environmental Context	Primary Noise Mechanism	Unconverged RMS Error	Technical Action
VES 39	Adjacent to 330 kV power transmission corridor	Electromagnetic inductive coupling and 50 Hz powerline harmonic noise	18.7%	Excluded
VES 103	Active agricultural drainage channel with steep bank slope	Lateral current refraction violating 1D horizontal-layer assumptions	24.3%	Excluded

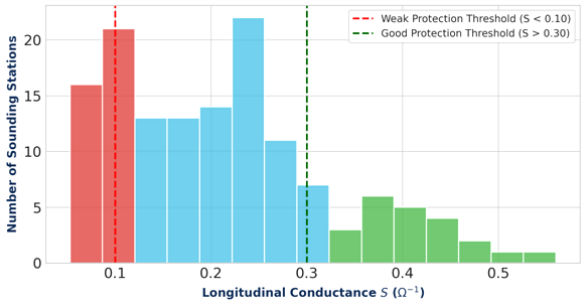

Figure 4: Histogram of Longitudinal Conductance (S) parameter distribution highlighting protective capacity zoning thresholds (Poor $< 0.1\ \Omega^{-1}$ versus Good $> 0.3\ \Omega^{-1}$).

4.2. Spatial distribution of Geo-Hydraulic and Dar Zarrouk parameters

The computed Dar-Zarrouk and hydraulic parameters exhibit distinct spatial variations across the study domain. As shown in the hydrogeophysical cross-plot in Figure 3, a strong, direct spatial relationship exists between aquifer layer thickness (haq) and computed transmissivity (Tr) across the 128 retained stations. Peaks in aquifer thickness (¿20 m) correspond directly to high-transmissivity zones (¿200 m²/day; Figure 3), highlighting structural sags within the Ogwashi–Asaba Formation that act as high-capacity regional storage conduits. Quantitatively, the estimated geo-hydraulic and Dar-Zarrouk parameters vary as follows:

1. **Transverse Resistance (T) and Transmissivity (T_r):** Computed T-values span 140.9 to 2048.6 $\Omega\,m^2$. As shown in Figure 3, stations with $T > 1000\ \Omega\,m^2$ yield empirical transmissivities ranging from 150 to 244.2 m^2/day. These high values confirm highly prolific sandstone units suitable for regional municipal supply schemes (Okonkwo & Emmanuel, 2026; Tom et al., 2026).
2. **Longitudinal Conductance (S) and Protective Vulnerability:** Computed S-values range from 0.053 to 0.560 Ω^{-1}. Figure 4 illustrates the frequency distribution of overburden protective capacity. According to standard Dar-Zarrouk protective vulnerability criteria (Oseji et al., 2023), stations exhibiting $S < 0.10\ \Omega^{-1}$ (Figure 4) indicate weak or poor protective clay cover, exposing underlying aquifers to surface agricultural and urban runoff. Conversely, stations with $S > 0.30\ \Omega^{-1}$ (Figure 4) possess robust clay/shale overburden, providing moderate-to-good natural protection against contaminant migration.

5. Conclusion and Recommendations

Re-validation of geoelectric field data across 128 VES stations, excluding the corrupted soundings (VES 39 and VES 103), delineated the hydrogeophysical architecture of the Ogwashi–Asaba and Ameki Formations. The key scientific findings from quantitative modelling and graphical analysis (Figures 1–4) are summarised as follows:

1. **Impact of Quality Control:** Figures 1 and 2 show that excluding VES 39 and VES 103 prevented severe artifacts from compromising regional contour mapping.
2. **Aquifer Productivity:** Figure 3 confirms substantial aquifer thicknesses (5.2–23.2 m) and high transmissivities of up to 244.2 m^2/day in structural sags.
3. **Vulnerability Zoning:** Figure 4 identifies key recharge zones characterised by thin overburden ($S < 0.1\ \Omega^{-1}$), which require strict environmental protection.

Recommendations: Future groundwater development should target high-transmissivity zones ($T > 1000\ \Omega\,m^2$; Figure 3), while environmental protection zones should be established around vulnerable areas characterised by low longitudinal conductance ($S < 0.1\ \Omega^{-1}$).

Conflict of interest

The authors declare there is no conflict of interest

Acknowledgements

This research was funded by the Tertiary Education Trust Fund (TETFund) through the Institution-Based Research (IBR) intervention line (Grant/Approval No.: TETF/DESS/UNIZIK/AWKA/IBR/2026/BATCH 20/VOL.1/46). The authors gratefully acknowledge TETFund for its financial support towards the successful completion of this study.

References

Chinyem, F. I., Abriku, E. O., Ovwamuedo, G., Salami, S. A., Igili, C. O., Nwugha, V. N., & Osieke, J. O. (2026). Hydrogeophysical

Table 2: Statistical Summary of Hydrogeophysical and Geo-Hydraulic Parameters across 128 Retained Stations

Parameter Name	Symbol (Units)	Minimum	Maximum	Mean $\pm$ Std. Dev.	Median
Aquifer Resistivity	ρ_{aq} (Ω·m)	27.1	108.9	67.4 ± 21.3	67.15
Aquifer Thickness	h_{aq} (m)	5.2	23.2	13.4 ± 5.6	13.45
Longitudinal Conductance	S (Ω^{-1})	0.053	0.560	0.218 ± 0.114	0.204
Transverse Resistance	T (Ω·m^2)	140.9	2048.6	954.2 ± 512.6	952.7
Hydraulic Conductivity	K (m/day)	5.69	14.05	8.24 ± 2.01	7.79
Transmissivity	T_r (m^2/day)	31.8	244.2	108.6 ± 51.4	107.8
Inversion RMS Error	RMS (%)	1.8	4.8	3.2 ± 0.8	3.1

investigation of groundwater potential, lithological strata and aquifer vulnerability in parts of Delta North District, Nigeria. *FUDMA Journal of Sciences*, 10(2), 375–389.

Ejije, C. E., & Atakpo, E. A. (2025). Delineation of subsurface lithology and aquifer structures using electrical resistivity surveys in parts of Ukwuani Local Government Area of Delta State. *Nigerian Journal of Science and Environment*, 23(1), 61–76. ISSN: 3043–4440.

Eyankware, M. O., Osisanya, O. W., Akakuru, O. C., Odesa, G. E., Okanigbuan, P. N., Ukor, K. P., Esi, E. O., & Chukwusa, F. O. (2025). Depiction of aquifer potential and vulnerability mapping: A case study of Delta North, Southern Part of Nigeria, using geophysical approach. *Discovery Nature*, 2, 1–16.

Heigold, P. C., Gilkeson, R. H., Cartwright, K., & Reed, P. C. (1979). Aquifer transmissivity from surficial electrical resistivity methods. *Groundwater*, 17(4), 338–345.

Loke, M. H., Dahlin, T., & Rucker, D. F. (2021). Smoothness-constrained time-lapse electrical resistivity tomography inversion with data re-validation. *Journal of Applied Geophysics*, 188, 104308.

Meju, M. A., & Abubakar, R. (2022). Quantitative geoelectric inversion and error analysis in complex sedimentary aquifers. *Journal of Environmental and Engineering Geophysics*, 27(3), 145–159.

Okonkwo, J. E., & Emmanuel, E. D. (2026). Appraisal of aquifer protective capacity and groundwater potential using the vertical electrical sounding technique in Illah, Delta State, Nigeria. *Al-Bahir: Journal for Engineering and Pure Sciences*, 8(1), 108–123.

Oseji, W. O., Egbai, J. C., & Okolie, E. C. (2023). Hydrogeophysical parameterization and Dar Zarrouk assessment of coastal aquifers in the Western Niger Delta. *Arabian Journal of Geosciences*, 16(5), 312.

Tom, C. N., Warmate, T., & Dieokuma, T. (2026). Quantitative assessment of aquifer transmissivity and vulnerability using Dar Zarrouk parameters from Schlumberger resistivity soundings in the Borikiri area, Niger Delta. *International Journal of Innovative Science and Research Technology*, 11(3), 3124–3130.